JOURNAL OF MATERIALS SCIENCE: MATERIALS IN MEDICINE 7 (1996) 309–316

The kinetics of calcium deficient and stoichiometric hydroxyapatite formation from $CaHPO_4 \cdot 2H_2O$ and $Ca_4(PO_4)_2O$

K. S. TENHUISEN, P. W. BROWN
Penn State University, Intercollege Materials Research Laboratory, University Park, PA 16802, USA

Isothermal calorimetry was performed on intimate mixtures of $CaHPO_4 \cdot 2H_2O$ and $Ca_4(PO_4)_2O$ constituted at Ca/P molar ratios of 1.50 and 1.67 to form the hydroxyapatite compositions $Ca_9HPO_4(PO_4)_5OH$ and $Ca_{10}(PO_4)_6(OH)_2$, respectively, at complete reaction. The temperature range investigated was 15–70 °C. The effects of the reaction temperature on the rates of heat evolution during hydroxyapatite formation were determined. Reactions were carried out utilizing a liquid-to-solids weight ratio of 1.0. A two-stage reaction mechanism was observed regardless of the Ca/P ratio as indicated by the presence of two reaction peaks in the plots of the rates of heat evolution against time. An Arrhenius relationship was found between the rate and temperature for each reaction stage for both compositions. Apparent activation energies of 120 and 90 kJ/mol (Ca/P = 1.67) and 118 and 83 kJ/mol (Ca/P = 1.50), respectively, were calculated for the first and second reaction peaks. An Arrhenius relationship was also found between the time of maximum rate and temperature. The following qualitative reaction mechanism is proposed for each of the two reaction stages for both compositions studied. The first stage involves the complete consumption of $CaHPO_4 \cdot 2H_2O$ and the partial consumption of $Ca_4(PO_4)_2O$ to form a noncrystalline calcium phosphate and nanocrystalline hydroxyapatite. During the second stage the remaining $Ca_4(PO_4)_2O$ reacts with the noncrystalline calcium phosphate to form the final product, stoichiometric or calcium deficient hydroxyapatite.

1. Introduction

Until recently calcium phosphate cements (CPC) formed by reactions between tetracalcium phosphate [$Ca_4(PO_4)_2O$ or TetCP] and an acidic calcium orthophosphate, such as dicalcium phosphate [$CaHPO_4$ or DCP], dicalcium phosphate dihydrate [$CaHPO_4 \cdot 2H_2O$ or DCPD], or MCPM [$Ca(H_2PO_4)_2 \cdot H_2O$] to form hydroxyapatite [$Ca_{10-x}(HPO_4)_x(PO_4)_{6-x}(OH)_{2-x}$ where $0 \leq x \leq 1$ or HAp] did not reach completion within clinically relevant periods of time without the use of accelerators [1–4]. Typically the kinetics and setting time of these reactions are accelerated [4–12] by the addition of either large proportions of HAp filler and/or by accelerating the reaction using acidic solutions (phosphoric acid, acetic acid, maleic acid, etc.).

Cementitious reactions between calcium orthophosphate salts to form HAp have many desirable properties for use in dentistry, orthopaedics, and reconstructive surgery. The compressive strength of HAp formed by low temperature cementitious reactions are equivalent to high temperature apatites with equal porosities reaching a value as high as 175 MPa [13]. Other studies have reported compressive strengths up to 51 MPa [14] and diametrial strengths of 12 MPa [14, 15] for castable CPCs. If constituted properly, these reactions result in solution conditions (i.e. pH and ionic strength) that would be unlikely to result in tissue damage to the surrounding tissue. For many *in vivo* applications it would be desirable to implant a formable putty-like material that would harden in place and form both a mechanical and chemical bond to the surrounding native tissue. Cementitious reactions to form monolithic HAp are ideal for such applications. Because HAp readily forms solid solutions which can incorporate various cationic and anionic species into its structure, low temperature formation allows HAp chemistry to be varied and thereby allows control of specific properties including surface area, microstructure, and crystallinity/crystallite size.

Establishing the relationships between the *in vitro* temperature dependence and the mechanistic reaction path(s) of these reactions is essential if HAp formed in this way is to be tailored for *in vivo* use. While a number of studies have investigated strength development and/or setting times of CPCs containing TetCP and DCP/DCPD [4, 5, 7, 9, 14, 16] an in-depth investigation and interpretation of the kinetics of these types of reactions has not been reported. The present investigation describes reactions between TetCP and DCPD proportioned to form both calcium deficient

0957–4530

(Ca/P = 1.50) and stoichiometric (Ca/P = 1.67) HAp. The apparent activation energies for these reactions are calculated and discussed. Finally, a qualitative reaction mechanism is proposed from the calorimetric data and X-ray diffraction [17] of the solids performed as a function of time. A similar study has been performed on the DCP/TetCP system [18].

2. Experimental procedure

2.1. Precursor synthesis

TetCP was synthesized by a high temperature solid state reaction between reagent grade monetite ($CaHPO_4$, Fisher Scientific) and precipitated calcium carbonate ($CaCO_3$, Fisher Scientific). Equimolar quantities of monetite and calcium carbonate were milled and then fired at 1400 °C for 2 h. The fired product was ground by hand and then milled to a particle size ~2.5 μm as determined by light scattering particle size analysis. X-ray diffraction was used to confirm phase purity. No evidence of hydroxyapatite or CaO was observed.

DCPD (300 g) was precipitated via an acid-base reaction between calcium hydroxide and monocalcium phosphate monohydrate (MCPM, $Ca(H_2PO_4)_2 \cdot H_2O$). Precipitated calcium carbonate (Fisher Scientific) was calcined at 1100 °C for 2 h to CaO and then ground in a mortar and pestle. A calcium hydroxide slurry was prepared by the addition of 48.435 g of CaO to 750 ml of deionized water in a sealed 1 l Nalgene bottle. This slurry was added to a slurry of 217.71 g of reagent grade MCPM (J.T. Baker) in 2250 ml of deionized water. The reactants were stirred for 15 min during which time DCPD was formed, then filtered through #5 Whatman filter paper. The precipitate was dispersed in acetone and again filtered to remove excess water. The precipitate was dried under vacuum (53 Pa) using a cold trap to capture the acetone. X-ray diffraction confirmed phase pure DCPD. No HAp was observed on the surfaces of the DCPD by scanning electron microscopy.

DCPD and TetCP were combined in 2-to-1 and 1-to-1 molar ratios and milled together to prepare HAp precursor powders with Ca/P molar ratios of 1.50 and 1.67, respectively. Equations 1 and 2 show the formation of calcium deficient (Ca/P = 1.50) and stoichiometric (Ca/P = 1.67) HAp from the above two powders.

$$6CaHPO_4 \cdot 2H_2O + 3Ca_4(PO_4)_2O \rightarrow 2Ca_9(HPO_4)(PO_4)_5OH + 13H_2O \quad (1)$$

$$2CaHPO_4 \cdot 2H_2O + 2Ca_4(PO_4)_2O \rightarrow Ca_{10}(PO_4)_6(OH)_2 + 4H_2O \quad (2)$$

2.2. Kinetics

The rates of formation of calcium deficient and stoichiometric HAp were measured using isothermal calorimetry at the following temperatures: 15, 20, 25, 30, 33.5, 37.4, 40, 45, 50, 55, 60, 65, and 70 °C. The HAp precursor powder (3.000 g) was placed in a copper calorimeter cup and deionized water (3.0 ml) was drawn into a 3 ml syringe. These were inserted into the calorimeter body and separately equilibrated. Upon thermal equilibration the water was injected into the calorimeter cup. A datum point was collected every 3 s and stored on a computer. Details of data collection and the system design have been previously discussed [19]. All rate and heat curves are plotted per mol of HAp formed. X-ray diffraction was used to confirm that all reactions had gone to completion.

3. Results and discussion

3.1. Isothermal calorimetry

3.1.1. Stoichiometric HAp

Isothermal calorimetry performed on DCPD–TetCP powders with a Ca/P molar ratio of 1.67 showed that the rate of stoichiometric HAp formation depended strongly on temperature (see Fig. 1). Complete reaction was reached between 0.5 and 36 h. Fig. 1 plots the heat evolved in kJ/mol of HAp formed at reaction temperatures from 15 to 70 °C. The total heat evolved is approximately the same in all experiments (290–300 kJ/mol). This combined with X-ray diffraction analyses of the product phases indicates that complete reaction was reached in each experiment.

Figs. 2 and 3 show calorimetric data for selected reaction temperatures (33.5 to 60 °C) to illustrate trends in the kinetics of HAp formation. Fig. 2 shows calorimetric curves that plot rates of HAp formation (dQ/dt versus t as watts/mol of HAp formed). Fig. 3 shows the corresponding heat evolution curves. These plot the total heats evolved (Q versus t in kJ/mol of HAp formed). The rate curves shown in Fig. 2 are characterized by two reaction peaks. When HAp formation is carried out at 33.5 °C a small mixing peak can be seen during the first few minutes after the injection of water. This results from the wetting of the

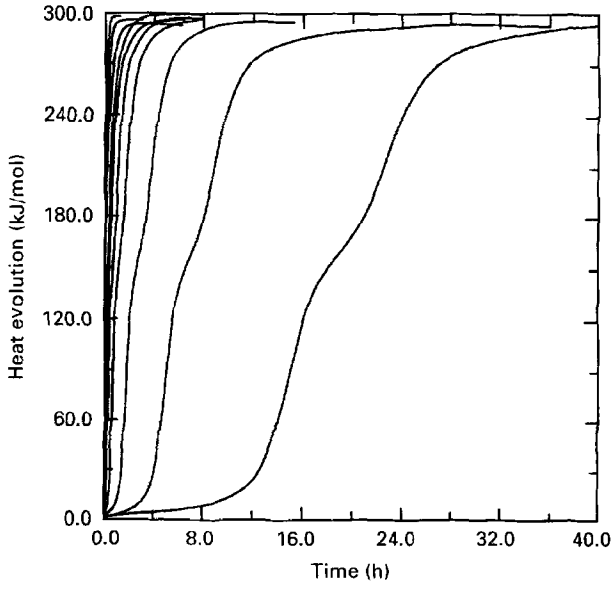

Figure 1 Heat evolution curves for the formation of stoichiometric hydroxyapatite from DCPD and TetCP over a temperature range of 15 to 70 °C illustrating the high temperature dependence of the reaction. The curves from right to left are for reaction temperatures of 15, 20, 25, 30, 33.5, 37.4, 40, 50, 60, and 70 °C.

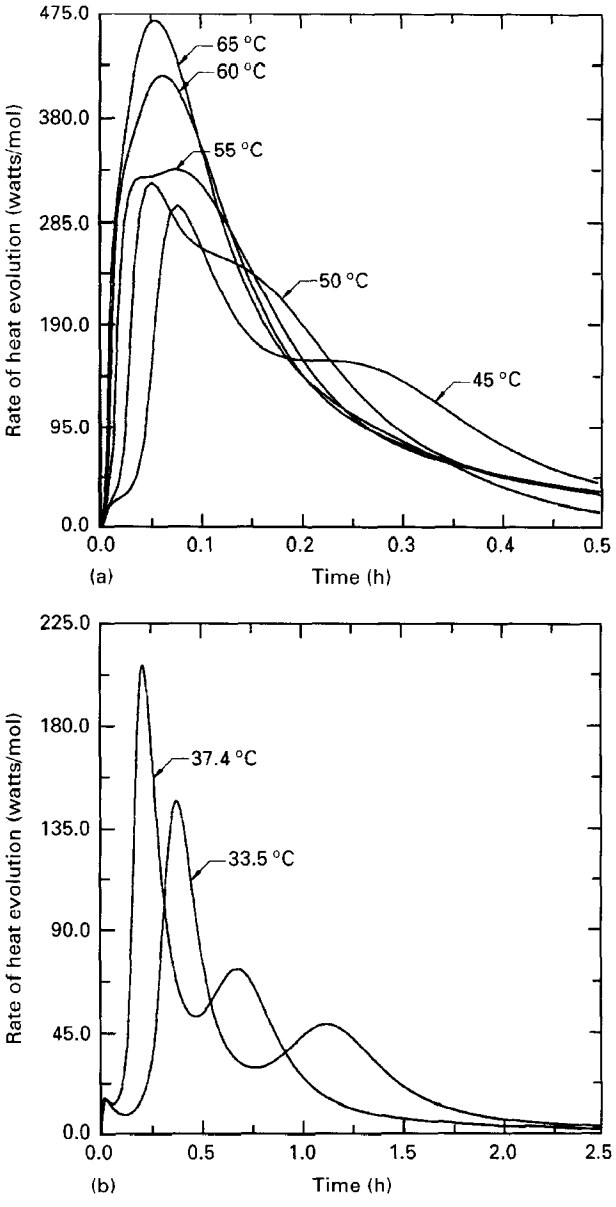

Figure 2 Rate curves for the formation of stoichiometric hydroxyapatite from DCPD and TetCP for selected reaction temperatures between 33.5 and 65 °C.

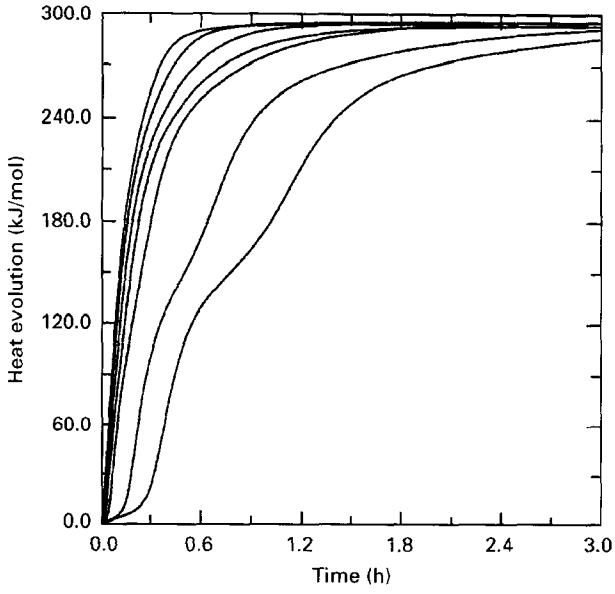

Figure 3 Heat evolution curves for the formation of stoichiometric hydroxyapatite from DCPD and TetCP for selected temperatures illustrating the two slopes resulting from two different reaction peaks in the rate curves. The curves from right to left are for reaction temperatures of 33.5, 37.4, 45, 50, 55, 60, and 65 °C.

reactant powder and is referred to as the heat of mixing. Subsequently, there is a period of slow reaction of about 10 to 15 min in duration. The first reaction peak then initiates and continues between about 15 and 45 min. A second reaction peak becomes apparent after about 45 min of reaction; the majority of heat associated with this peak (~95%) is evolved by 3 h with the reaction reaching completion within approximately 5 h (see Figs. 1 and 3).

At higher temperatures these reaction peaks occur at shorter times. By 45 °C the first reaction peak overlaps the mixing peak and the two are no longer separable. As the reaction temperature increases the two reaction peaks increasingly overlap (see Fig. 2). By 50 °C the second reaction peak becomes a shoulder on the first. As the temperature is further increased to 55–60 °C, the first reaction peak becomes a shoulder on the second reaction peak. By 65 °C the first reaction peak can no longer be observed and the only predominant feature is the second peak.

The features described with reference to Fig. 2 are again evident in the integral curves (Figs. 1 and 3). Induction periods and two slopes are observed up to 45 °C. Two slopes in the heat curves are difficult to discern at higher temperatures due to the increasing overlap of the two reaction peaks as the temperature is increased. Fig. 3 shows that the total heat evolved is a constant of about 295 kJ/mol of HAp formed. This is indicative of complete reaction. It was not possible to achieve complete reaction in our earlier studies in the absence of extended periods of slow reaction [2].

As indicated by the two reaction peaks in the rate curves and resulting two slopes in the heat curves, HAp formation occurs in two mechanistic steps. The inflection points on the heat curves (Figs. 1 and 3) between the first and second reaction peaks occur at approximately the same heat output (~150–160 kJ/mol) regardless of the reaction temperature. This indicates that the area under each reaction peak in the rate curves (Fig. 2), if deconvoluted, is approximately the same for all reaction temperatures studied. X-ray diffraction studies on solids present as a function of time and reaction temperature [17] and the above calorimetric results indicate that the same two reaction mechanisms are associated with the two reaction peaks over the temperature range studied.

X-ray diffraction analyses shows the consumption of DCPD precedes that of TetCP at 25.0, 37.4, and 50.0 °C [17]. As the temperature of HAp formation is increased, the time between the disappearance of DCPD and that of TetCP diminishes. This correlates with the increasing overlap of the two reaction peaks as the temperature is increased. The disappearance of DCPD occurs after the maxima of the first reaction peak but before the minima between the first and second peaks (~0.4 h at 37.4 °C and ~2.1 h at 25.0 °C). At this time, X-ray diffraction analyses indicates the presence of TetCP, small crystallites of HAp, and an amorphous-like background suggestive of a noncrystalline calcium phosphate (NCP) [17].

Amorphous calcium phosphates have been shown to be an intermediate product in the precipitation of HAp in a number of studies [20–26]. Transmission electron microscopy on the solids present after the calorimetric studies were completed indicates the presence of two reaction products; HAp and one that is amorphous by electron diffraction [27] indicating the presence of an intermediate NCP phase even after complete reaction as observed by calorimetry and X-ray diffraction. Thus the intermediate products appear to be a mixture of two phases; nanocrystallite HAp and a NCP that is not necessarily of a fixed composition [23, 32–35]. Octacalcium phosphate ($Ca_8(HPO_4)_2(PO_4)_4 \cdot 5H_2O$ or OCP) has been reported to form as an intermediate in the synthesis of HAp [28–31]. However, OCP was not detected by X-ray diffraction at any stage of reaction. A qualitative reaction mechanism for the first stage of the reaction is shown in Equation 3.

$$2CaHPO_4 \cdot 2H_2O + (2 - x)Ca_4(PO_4)_2O \rightarrow \text{NCP } (1.2 \leq Ca/P \leq 1.5) + \text{HAp } (1.50 \leq Ca/P \leq 1.67) \quad (3)$$

This expression applies when HAp formation is rate limited by the reactivity of the basic phase because all reactions investigated in this study were limited in rate by TetCP. Although X-ray diffraction analysis shows that the DCPD is consumed prior to the TetCP, the proportion of TetCP reacted is not easily determined due to the presence of a nanocrystalline HAp and an amorphous phase. This in combination with the variable composition of the two product phases that form during the first reaction step precludes the determination of a balanced Equation 3. Therefore, the variable x allows for the formation of an intermediate phase(s) with variable Ca/P ratios. Such variability depends on the relative rates of DCPD and TetCP dissolution. This depends in turn on the methods of preparation and particle size of the reactants and the reaction temperature.

Equation 4 shows the second mechanistic step to be the reaction of the intermediate phase(s) formed in association with the first calorimetric reaction peak, Equation 3, with the remaining TetCP (x) in the formation of stoichiometric HAp. The heat evolved during this reaction causes the second calorimetric reaction peak.

$$xCa_4(PO_4)_2O + \text{NCP}(1.2 \leq Ca/P \leq 1.5) + \text{HAp}(1.50 \leq Ca/P \leq 1.67) \rightarrow Ca_{10}(PO_4)_6(OH)_2 \quad (4)$$

As previously mentioned the quantity of heat produced by each of the two reaction stages appears to remain nearly constant regardless of the temperature. This suggests that the relative quantities of the intermediate(s) should be nominally constant, regardless of the reaction temperature. Thus, the only difference resulting from a change in the temperature at which HAp forms is the extent of the overlap of the two reaction steps. As will be discussed, a similar mechanistic path is followed in the formation of calcium deficient HAp.

3.1.2. Calcium deficient HAp

The mechanistic steps during the formation of calcium deficient HAp (Ca/P = 1.50) from DCPD and TetCP are similar to those observed for stoichiometric HAp formation. Fig. 4 shows heat curves for calcium deficient HAp for selected reaction temperatures between 15 and 70 °C. Complete reaction was reached between approximately 0.5 and 28 h. All reactions evolve approximately the same quantity of heat upon completion (240 kJ/mol of HAp formed), again indicating that complete reaction was achieved at all the temperatures studied.

Figs. 5 and 6 shows calorimetric data at selected reaction temperatures (33.5 to 65 °C) to illustrate trends in the kinetics of calcium deficient HAp formation. Two discenable slopes are again present in the heat curves as a result of the two reaction peaks in the rate curves. These data indicate a two-stage reaction mechanism. As will be discussed in the following section, these two reaction peaks appear to overlap to a greater extent at any given reaction temperature than during the formation of stoichiometric HAp.

At 33.5 °C a mixing peak is again observed (see Fig. 5) upon injection of the water. A short induction period of approximately 5 to 10 min is also apparent. The first reaction peak occurs between about 10 min and 45 min. The second reaction peak becomes apparent at about 45 min and proceeds until the reaction has reached completion after about 2.5 h. There is no induction period when HAp is formed at temperatures $\geq$ 45 °C and a distinct mixing peak cannot be discerned as the reaction initiates immediately upon injection of the water. As the reaction temperature is increased the two reaction peaks again increasingly overlap, and at temperatures greater than 45 °C they become indiscernable.

X-ray diffraction analyses again shows the disappearance of DCPD prior to TetCP resulting in the

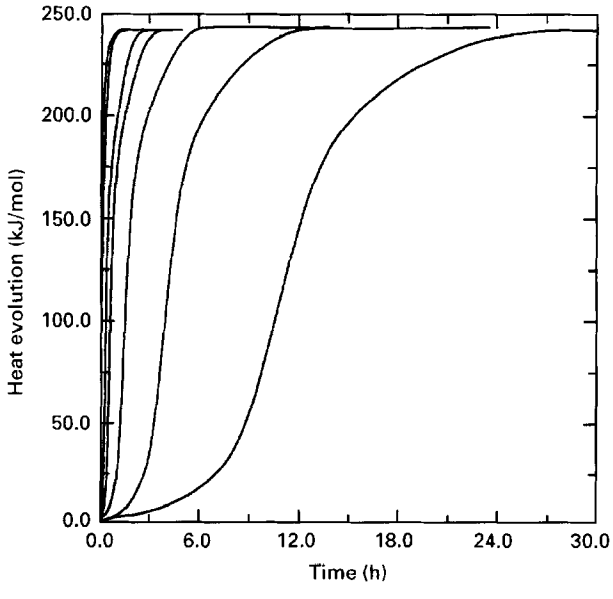

Figure 4 Heat evolution curves for the formation of calcium deficient hydroxyapatite from DCPD and TetCP over a temperature range of 15 to 70 °C illustrating the high temperature dependence of the reaction. The curves from right to left are for reaction temperatures of 15, 20, 25, 30, 33.5, 37.4, 40, 50, 60, and 70 °C.

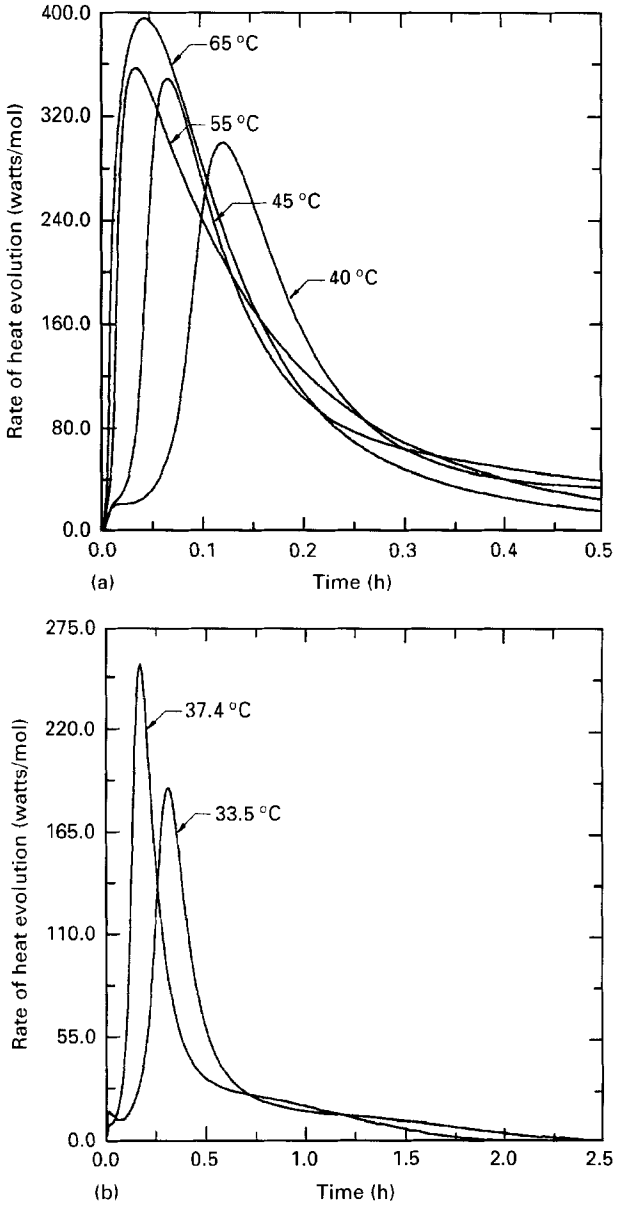

Figure 5 Rate curves for the formation of calcium deficient hydroxyapatite from DCPD and TetCP for selected reaction temperatures between 33.5 and 65 °C.

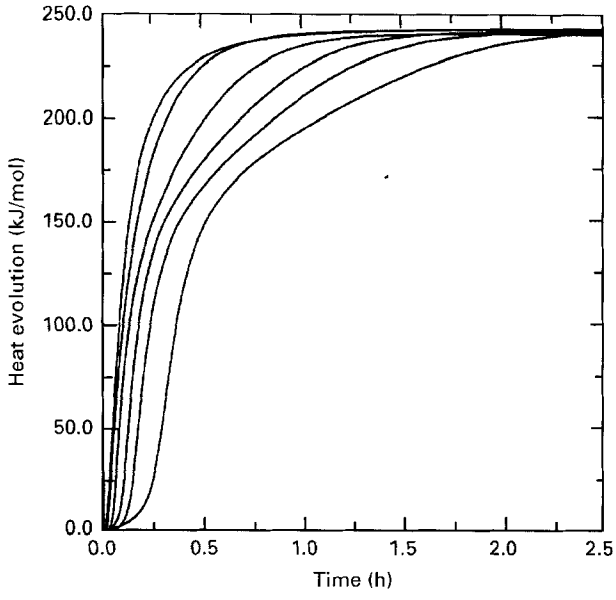

Figure 6 Heat evolution curves for the formation of calcium deficient hydroxyapatite from DCPD and TetCP for selected temperatures illustrating the two slopes resulting from two different reaction peaks in the rate curves. The curves from right to left are for reaction temperatures of 33.5, 37.4, 40, 45, 55, and 65 °C.

formation of intermediate phases [17, 27]. As the temperature is increased, the time between the disappearance of DCPD and complete reaction (disappearance of TetCP) decreases. This correlates with the increasing overlap of the two reaction peaks. Again the disappearance of DCPD occurs after the maxima of the first reaction peak (~0.6 h at 37.4 °C and ~2.4 h at 25.0 °C). As in the formation of stoichiometric HAp there are indications of the presence of an amorphous phase [17, 27]. A qualitative reaction mechanism for the first reaction peak is shown in Equation 5.

$$6CaHPO_4 \cdot 2H_2O + (3 - x)Ca_4(PO_4)_2O \rightarrow$$
$$NCP\ (1.2 \leq Ca/P \leq 1.5) +$$
$$HAp\ (1.50 \leq Ca/P \leq 1.67) \quad (5)$$

As in the formation of stoichiometric HAp, the reactivity of the TetCP is rate limiting even though there is relatively more DCPD precursor. The use of the variable x again represents the rate limiting nature of the basic reactant phase and shows that the DCPD is consumed prior to the TetCP. The reaction corresponding to the second reaction peak is shown in Equation 6, where the previously formed HAp/NCP intermediate phases react with the remaining TetCP to form calcium deficient HAp.

$$xCa_4(PO_4)_2O + NCP(1.2 \leq Ca/P \leq 1.5) +$$
$$HAp\ (1.50 \leq Ca/P \leq 1.67) \rightarrow$$
$$Ca_9(HPO_4)(PO_4)_5OH \quad (6)$$

The formation of OCP was not detected for X-ray diffraction kinetic studies at 25.0, 37.4, and 50.0 °C [17].

3.2. Relationships in DCPD/TetCP reactions

An Arrhenius plot (Fig. 7) can be obtained by plotting the natural log of the normalized maximum reaction rate for each of the two reaction peaks as a function of the inverse of temperature (Kelvin). An apparent activation energy value (E_{act}) can be calculated for each of the two stages of reaction for both calcium deficient and stoichiometric HAp. These values are shown in Table I. These values indicate that both reaction steps exhibit a high temperature dependence and are controlled by nucleation and growth mechanisms. The E_{act} for the first reaction peak is nominally constant (118–120 kJ/mol), regardless of the composition. This suggests that the relative changes in congruency and solubility of the precursors remain the same as the temperature varies. Therefore, the temperature dependence of the hydrolysis of the TetCP is the same regardless of the TetCP-to-DCPD ratio, and the TetCP is rate limiting precursor over the entire temperature and composition range. The E_{act} for the second reaction peak differs with composition; it is higher for the calcium deficient composition. This suggests

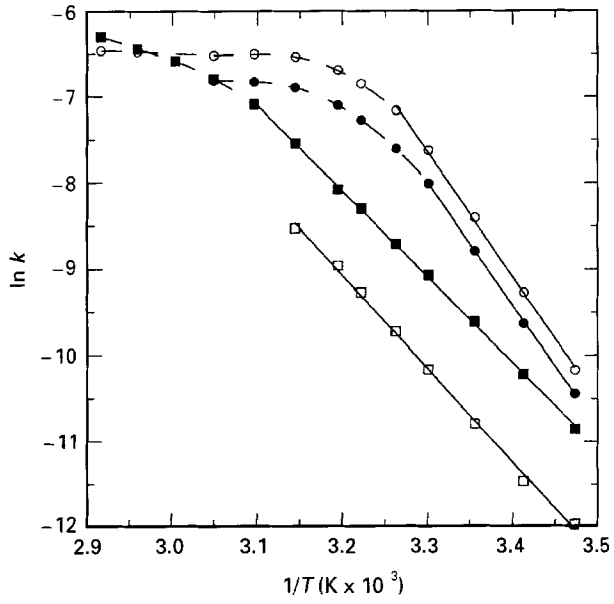

Figure 7 Arrhenius plot of the rate (k) of the first and second reaction peaks of both stoichiometric and calcium deficient hydroxyapatite formation from DCPD and TetCP. The solid lines represent the linear region of the Arrhenius relationship. (○ first reaction peak, □ second reaction peak; open data points correspond to calcium deficient HAp, and filled data points correspond to stoichiometric HAp).

that there is a higher temperature dependence for the reaction of the intermediates than for the remaining TetCP. It is probable that both the proportions of HAp and NCP and their composition differ between the stoichiometric and calcium deficient stoichiometries. This is supported by calorimetric results showing that the first reaction peak for the calcium deficient composition evolves a greater quantity of heat than does the stoichiometric composition (~190 kJ/mol versus 155 kJ/mol). If the composition and quantities of the NCP and HAp intermediate phases were identical, regardless of bulk composition, the quantity of heat produced by the first reaction peak should also be the same.

The times to reach complete reaction also change with composition. At lower temperatures, the formation of stoichiometric HAp takes longer times to reach completion. As the temperature is increased the stoichiometric mixture requires increasingly less time to reach completion with respect to calcium deficient HAp. By about 55 °C, times to complete reaction are nominally the same for the two compositions, and at temperatures of 65 to 70 °C the formation of calcium deficient HAp requires more time to reach completion. This indicates that the intermediates formed may actually become the rate limiting phase(s) during the second reaction mechanism as the temperature is increased.

A noticeable difference between the calorimetric data for stoichiometric and calcium deficient HAp formation is that the maximum rate (peak height) for the first reaction peak at any temperature is higher for calcium deficient than for stoichiometric compositions. This trend further supports the first reaction stage mechanism previously proposed. Another compositional difference is the degree of overlap of the two reaction peaks at any temperature (see Figs. 2 and 5). There is a much greater overlap in the formation of calcium deficient HAp as a result of a lower proportion of the rate limiting reactant phase, TetCP. A lower proportion of TetCP also results in less heat evolution during the second reaction stage in calcium deficient HAp formation. This results in a lower maximum rate (peak height) at any given temperature. By 50.0 °C the extent of overlap becomes so great that the two peaks can no longer be discerned. Because of this the activation energy for the second reaction peak was calculated using temperatures from 15 and 45 °C for calcium deficient HAp. Conversely, for stoichiometric HAp the first reaction peak becomes a shoulder by 60 °C (see Fig. 2a) and its activation energy curve is only calculated from 15 to 55 °C.

Three of the curves in Fig. 7 deveate from linearity at the higher reaction temperatures. This is a result of the relatively long time constant (4.6×10^{-2} h) of the calorimeter [18, 19]. Nonlinearity results from heat transfer limitations as a consequence of the heat capacity of the solids and the extremely high kinetics at the elevated reaction temperatures. The deviation from linearity occurs when the natural log of the rate constant reaches a value of approximately -7.5 to -7.0 corresponding to a rate of 250–300 watts/mol.

The times at which the maximum rate occurs for these reactions also exhibit an exponential relationship. The natural log of the time of the maximum rate (peak height) is plotted versus $1/T$ for three of the four reaction peaks observed in this investigation (see Fig. 8). Due to the reaction peak overlap and the broadness of the second reaction peak for calcium deficient HAp formation, these times were not plotted. At lower temperatures a linear relationship is observed and an apparent activation value was obtained for the time dependence of the peak on reaction temperature (see Table I). The times of the first reaction peaks maximum exhibit a high temperature dependence with an E_{act} of approximately 135–140 kJ/mol. The times of the second reaction peak maximum for stoichiometric HAp formation shows a lower temperature dependence than the first peak, with an E_{act} of 115 kJ/mol.

TABLE I Activation energy, E_{ACT}

Ca/P ratio	1st reaction peak (maximum rate) (kJ/mol)	2nd reaction peak (maximum rate) (kJ/mol)	1st reaction peak (time of maximum rate) (kJ/mol)	2nd reaction peak (time of maximum rate) (kJ/mol)
1.50	120.1	90.4	134.3	–
1.67	118.1	82.7	138.8	114.7

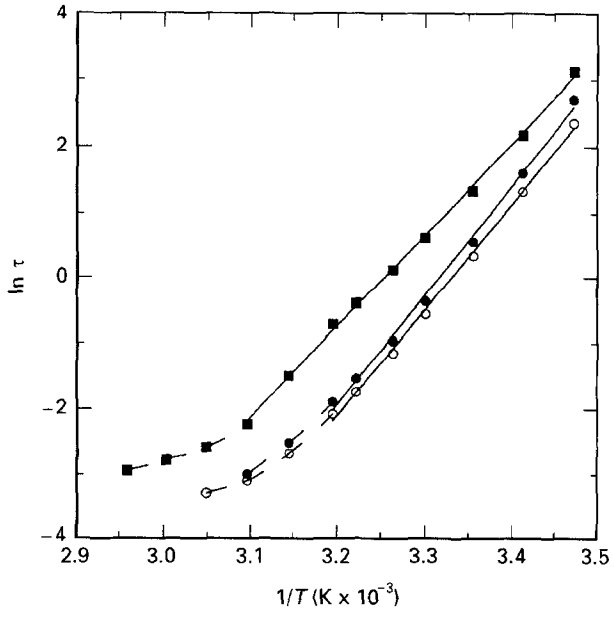

Figure 8 Arrhenius plot of the time of maximum rate (τ) of the first reaction peak of calcium deficient hydroxyapatite formation and the first and second reaction peaks of stoichiometric hydroxyapatite formation from DCPD and TetCP. The solid lines represent the linear region of the Arrhenius relationship. (○ first reaction peak, □ second reaction peak; open data points correspond to calcium deficient HAp, and filled data points correspond to stoichiometric HAp).

The kinetics of HAp formation from DCPD and TetCP are complicated by the retrograde solubility of DCPD and HAp [36, 37]. A further factor complicating the kinetics is that DCPD dissolves incongruently. This results in the overgrowth of DCPD with HAp. TetCP is not stable in aqueous solutions and will react over time to form HAp and $Ca(OH)_2$ [38–40]; however, without mechanical agitation, such as continuous milling or ultrasonic agitation, it will also become overgrown with HAp. As a consequence hydrolysis of DCPD and TetCP can become diffusionally controlled. The increase in reaction rate with temperature for HAp formation from DCPD and TetCP in this study occurs because the intimacy of mixing minimizes the effects of the overgrowth of the reactant phases by HAp. Reactions between TetCP and DCPD displaying slower kinetics than in the present study reach a maximum reactivity with increasing temperature and would eventually display a decrease in reactivity as the temperature was further increased resulting in longer times to complete reaction as was previously observed [3].

4. Conclusions

Reactions between DCPD and TetCP over a temperature range of 15–70 °C to form both stoichiometric (Ca/P = 1.67) and calcium deficient (Ca/P = 1.50) HAp display a two-step reaction path. This is indicated by the presence of two peaks in the calorimetric curves showing the rates of heat evolution with time. The first reaction step involves the consumption of all DCPD and some of the TetCP to form an intermediate NCP phase and small crystallites of HAp. The second step involves the reaction between the intermediate phases and the remaining TetCP.

The quantity of heat evolved under each reaction peak for each bulk composition remained nominally constant with temperature. The two reaction peaks increasingly overlapped one another as the reaction temperature increases until the second and first reaction peaks, respectively, become unresolvable for the formation of calcium deficient and stoichiometric HAp. At low temperatures complete reaction to stoichiometric HAp requires longer times than does calcium deficient HAp due to the presence of greater quantities of TetCP. At temperatures above 55–60 °C formation of calcium deficient HAp requires more time than does stoichiometric HAp. This likely results from differences in both the proportions and compositions of the intermediate phases that form as indicated by the differences in the quantities of heat evolved by the first reaction peak with bulk composition.

The apparent activation energy for both reaction steps in HAp formation indicate a high apparent activation consistent with a nucleation and growth mechanism. A lower temperature dependence was associated with the second reaction step. An Arrhenius relationship was also shown between the time of maximum rate and reaction temperature.

Acknowledgements

The authors would like to thank the National Institute of Health, grant #DE09421, for financial support.

References

1. P. W. BROWN, N. HOCKER and S. HOYLE, *J. Amer. Ceram. Soc.* **74** (1991) 1848.
2. M. T. FULMER and P. W. BROWN, *ibid.* **74** (1991) 934.
3. M. T. FULMER and P. W. BROWN, *J. Mater. Res.* **8** (1993) 1687.
4. W. E. BROWN and L. C. CHOW, in "Cements research progress," edited by P. W. Brown (American Ceramic Society, Westerville, OH, 1987) p. 352.
5. L. XIE and E. A. MONROE, in "Materials Research Society Symposium Proceedings" Vol. 179, edited by B. Sheetz, A. Landers, I. Odler, and H. Jennings (Materials Research Society, Pittsburgh, PA, 1991) p. 25.
6. M. S. TUNG, N. EIDELMAN, B. SIECK and W. E. BROWN, *J. Res. Natn. Bur. Stands.* **93** (1988) 613.
7. L. C. CHOW, S. TAKAGI, P. D. CONSTANTINO and C. D. FRIEDMAN, in "Materials Research Society Proceedings," Vol. 179, edited by B. Sheetz, A. Landers, I. Odler, and H. Jennings (Materials Research Society, Pittsburgh, PA, 1991) p. 3.
8. Y. DOI, Y. TAKEZAWA, S. SHIBATA, N. WAKAMATSU, H. KAMEMIZU, T. GOTO, M. IIJIMA, Y. MORIWAKI, K. UNO, F. KUBO and Y. HAEUCHI, *J. Jpn. Soc. Dent. Mater. Devices* **6** (1987) 53.
9. Y. TAKEZAWA, Y. DOI, S. SHIBATA, N. WAKAMATSU, T. GOTO, M. IIJIMA, Y. MORIWAKI, K. UNO, F. KUBO and Y. HAEUCHI, *ibid.* **6** (1987) 426.
10. N. EIDELMAN, L. C. CHOW and W. E. BROWN, *Calcif. Tissue Int.* **41** (1987) 18.
11. W. E. BROWN, N. EIDELMAN and B. TOMAZIC, *Adv. Dent. Res.* **1** (1987) 307.
12. K. S. TENHUISEN and P. W. BROWN, *J. Mater. Sci. Mater. Med.* **5** (1994) 291.
13. R. I. MARTIN and P. W. BROWN, *ibid.* **6** (1995) 138.

14. R. P. LINK, S. TAKAGI, S. GREENHUT, L. C. CHOW and R. L. STRAUSBERG, *J. Dent. Res.* (special issue) **70** (1991) 567 (abstract no. 2410).
15. N. SANIN, S. TAGAGI, L. C. CHOW and S. MATSUYA, *ibid.* **70** (1991) 567 (abstract no. 2411).
16. Y. FUKASE, E. D. EANES, S. TAKAGI, L. C. CHOW and W. E. BROWN, *ibid.* **69** (1990) 1852.
17. K. S. TENHUISEN and P. W. BROWN, *J. Bio. Mater. Res.* (submitted).
18. R. I. MARTIN and P. W. BROWN, *ibid.* (submitted).
19. E. J. PROSEN, P. W. BROWN, G. FROHNSDORFF and F. DAVIS, *Cem. Concr. Res.* **15** (1985) 703.
20. E. D. EANES, I. H. GILLESSEN and A. S. POSNER, *Nature* **208** (1965) 233.
21. E. D. EANES and A. S. POSNER, *Trans. N.Y. Acad. Sci.* **28** (1965) 233.
22. E. D. EANES, J. D. TERMINE and M. U. NYLEN, *Calcif. Tissue Res.* **12** (1973) 143.
23. C. HOLT, M. J. J. M. VAN KEMENADE, J. E. HARRIES, L. S. NELSON, R. T. BAILEY, D. W. L. HUKINS, S. S. HASNAIN and P. L. DE BRUYN, *J. Cryst. Growth* **92** (1988) 239.
24. A. L. BOSKEY and A. S. POSNER, *J. Phys. Chem.* **77** (1973) 2313.
25. A. S. POSNER, *Physiol. Rev.* **49** (1969) 760.
26. J. D. TERMINE and A. S. POSNER, *Science* **153** (1966) 1523.
27. K. S. TENHUISEN, B. CLARK, M. KLIMKIEWICZ and P. W. BROWN, *Cell and Materials* (submitted).
28. G. H. NANCOLLAS and B. TOMAZIC, *J. Phys. Chem.* **78** (1974) 2218.
29. B. TOMAZIC and G. H. NANCOLLAS, *J. Coll. Interface Sci.* **50** (1975) 451.
30. W. E. BROWN, J. P. SMITH, J. R. LEHR and W. A. FRAZIER, *Nature* **196** (1962) 1050.
31. B. TOMAZIC, M. TOMSON and G. H. NANCOLLAS, *Arch. Oral Biol.* **20** (1975) 803.
32. J. D. TERMINE and E. D. EANES, *Calcif. Tissue. Res.* **10** (1972) 171.
33. P.-T. CHENG and K. P. H. PRITZKER, *Calcif. Tissue Int.* **35** (1983) 596.
34. F. ABBONA, H. E. LUNDAGER MADSEN and R. BOISTELLE, *J. Crystal Growth* **74** (1986) 581.
35. C. HOLT, M. J. J. M. VAN KEMENADE, L. S. NELSON JR., D. W. L. HUKINS, R. T. BAILEY, J. E. HARRIES, S. S. HASNAIN and P. L. de BRUYN, *Mater. Res. Bull.* **23** (1989) 55.
36. T. M. GREGORY, E. C. MORENO and W. E. BROWN, *J. Res. Nat. Bur. Stand.* **74A** (1970) 461.
37. H. McDOWELL, T. M. GREGORY and W. E. BROWN, *ibid.* (1977) 273.
38. R. I. MARTIN and P. W. BROWN, *Adv. Cement Res.* **5**(19) (1993) 119.
39. L. XIE and E. A. MONROE, in "Handbook of bioactive ceramics, Vol. II, calcium phosphate and hydroxylapatite ceramics," edited by T. Yamamur, L. L. Hench and J. Wilson (CRC Press, Boca Raton, FL, 1990) p. 29.
40. E. C. CORBRIDGE, in "Phosphorus: an outline of its chemistry, biochemistry and technology," 3rd Edn (Elsevier, Amsterdam, 1985) p. 138.

Received 13 June
and accepted 23 September 1995